

Solar Neutrino Limits on Decoherence

P. C. de Holanda

September 23, 2019

Abstract

The solar neutrino flux arrives at Earth as an incoherent admixture of mass eigenstates, and then solar neutrino detection constitute a blind probe to the oscillation pattern of the neutrino flavour conversion. Consequently, it is also impossible to probe, in a model independent approach, any new physics that leads to an enhancement of decoherence during the neutrino evolution, an effect that is present for instance in Open Quantum System formalism. However, such mechanism can also induce changes between mass eigenstates if an energy interchange between the neutrino subsystem and the reservoir is not explicitly forbidden. In this work the conversion probabilities between mass eigenstates in an Open Quantum System are calculated, and limits are established for these kind of transitions. We present our results in a pedagogical way, pointing out how far the analysis can go without any assumption on the neutrino conversion physics inside the Sun, before performing the full calculations. We obtain as limits for the decoherence parameters the values of $\Gamma_3 < 6.5 \times 10^{-19}$ eV and $\Gamma_8 < 7.1 \times 10^{-19}$ eV at 3σ .

1 Introduction

The suppression in the total flux of solar neutrinos in comparison with the theoretical predictions provided the first indication of neutrino flavour conversion. The first results of the Homestake experiment already indicated that the observable flux of electron neutrinos arriving from the Sun were in clear disagreement with the solar models predictions at the time [1,2], a result that was later confirmed by a number of other experiments. Sage [3] in 1991

and Gallex [4] in 1992, Kamiokande [5] in 1988 and Super-Kamiokande [6] in 1998 and SNO [7] in 2001, all confirmed the suppression on the electron neutrino flux in different parts of the solar neutrino spectrum, while confirming the main features of the Standard Solar Model.

The flavour conversion induced by a non-vanishing neutrino mass and a mixing matrix relating flavour and mass eigenbasis was the first proposed solution to such discrepancy [8]. It soon became clear that neutrino interactions with solar matter would have a fundamental role on its flavour conversion through resonant amplification, the so-called MSW effect [9–11]. But several other mechanisms could also provide flavour conversion compatible with the data, and by the end of the 90's there were a number of possible solutions (see, for instance [12] for a comprehensive comparison between possible explanations for the solar neutrino problem).

Only in 2002 the results from KamLAND [13], a reactor neutrino detector, confirmed the mass induced flavour conversion of solar neutrinos. Located at Kamioka mine, KamLAND detected electron anti-neutrinos created in several different nuclear reactors on Japan's territory. Its results were compatible with flavour neutrino oscillations with oscillation parameters compatible with the solution to the solar neutrino problem based on resonant conversion with a large mixing angle - LMA. Several recent results confirm such scenario with great precision (see for instance [14] and [15] for comprehensive oscillation results analyses).

As usually happens with scientific explanations, the correct chronology of the events are not always the most pedagogical one. In nowadays is more straightforward to invert the chronology and present the oscillation phenomena starting with the vacuum oscillations observed by accelerator and reactor experiments, such as KamLAND, and using the solar neutrinos as an a-temporal comprovement of KamLAND's result.

In accordance with this pedagogical strategy, in this paper I present an exercise on how much information we can extract on solar neutrino flux independent of the flavour conversion mechanisms that operates inside the Sun. Departing from the safe assumption that the solar neutrino flux arrives at Earth as an incoherent admixture of mass eigenstates, I analyze what can be inferred about the fraction of each eigenstate in the total flux for different neutrino energies, using only information from the allowed regions for neutrino oscillation parameters provided by terrestrial experiments such as KamLAND [16] for the neutrino parameters θ_{12} and Δm_{21}^2 and Daya-Bay [17], Reno [18] and Double-Chooz [19] for the neutrino parameter θ_{13} ,

besides the predictions for the total solar neutrino flux and spectrum [20,21].

The knowledge of the solar neutrino flavour conversion mechanism inside the Sun clearly allows a more comprehensive analysis, but this may not be the case with other astrophysical environments that produces neutrinos. We then use the exercise presented here to extrapolate how other neutrino astrophysical sources could be analysed.

In section 2 we infer by present experimental data on solar neutrinos what information can be extracted about the solar neutrino flux partition between mass eigenstates, for low energy and high energy neutrinos. In section 3 we compute the effect of Open Quantum System formalism on neutrino conversion probabilities. In section 4 I obtain a limit on relaxation effects induced by open quantum system formalism, both independent from any consideration about the neutrino physics operating inside the Sun, and assuming the MSW-LMA conversion. Finally, I propose that similar procedures can be used to analyse astrophysical neutrinos, where the uncertainties on the flavour conversion mechanisms inside the neutrino astrophysical source are considerably greater than for solar neutrinos. In section 5 I draw the conclusions.

2 Solar Neutrino's Flux Constraints

The solar neutrino flux arrives at the Earth detectors as a complete incoherent admixture of mass eigenstates. Any coherence is lost due to three effects that solar neutrinos are subjected [22]:

- the average over the neutrino production point inside the sun;
- the fast oscillation on energy;
- the wave package decoherence induced by neutrino evolution.

Then, due to decoherence, the solar neutrino flavour conversion probabilities can be written as:

$$P_{e\beta} = \sum_i P_{ei}^{Sun} P_{i\beta}^{Earth} \quad (1)$$

where P_{ei}^{Sun} is the probability that an electron neutrino produced in the sun interior arrives at the Earth as eigenstate i , while $P_{i\beta}^{Earth}$ is the probability of detecting a neutrino that arrives at Earth as eigenstate i as flavour β . In

this section we extract the possible values for P_{ei}^{Sun} from the available solar neutrino data.

2.1 Neutrino's flavour survival probabilities

As it has been done in qualitative analysis regarding solar neutrinos, it is convenient to analyse the neutrino probabilities in three different energy ranges, low, medium and high energy neutrinos.

2.1.1 high energy:

The high energy neutrino flux consists mainly of Boron neutrinos, and the flux can be determined by experiments Super-Kamiokande [23–25] and SNO [26]. Under the assumption that the high-energy neutrino flux ($E \gtrsim 5$ MeV) is well described by a constant electron neutrino survival probability, the solar data allows to establish a value for such probability fitting the data from the different Super-Kamiokande and SNO phases. Using only the data corresponding to neutrinos arriving at the detectors during the day, the following χ^2 can be used:

$$\chi^2(f_B, P_{ee}) = \chi_{SK}^2(f_B, P_{ee}) + \chi_{SNO}^2(f_B, P_{ee}) \quad ,$$

where f_B is a free normalization factor for the Boron neutrino flux.

The Super-Kamiokande χ^2 is given by:

$$\chi_{SK}^2(f_B, P_{ee}) = \left[\sum_{ij} (f_B R_{SK}^{th,i} - R_{SK}^{exp,i}) [\sigma_{SK}]^{-2} (f_B R_{SK}^{th,j} - R_{SK}^{exp,j}) \right]$$

where the sum covers data from all Super-Kamiokande runs, and σ_{SK} entails all uncertainties and correlations. By itself Super-Kamiokande daily data can not provide any information on f_B and P_{ee} , since there is an almost perfect correlation between both variables.

SNO collaboration already presents their results in terms of survival probabilities, parametrized by 6 parameters: 3 regarding the parameterization of the daily probability P_{ee}^d , 2 regarding the regeneration effect A_{ee} , and 1 regarding neutral current measurement of total neutrino flux, which can be associated with the free normalization f_B mentioned above:

$$P_{ee}^d(E_\nu) = c_0 + c_1(E_\nu[MeV] - 10) + c_2(E_\nu[MeV] - 10)^2$$

$$\begin{aligned}
A_{ee}(E_\nu) &= a_0 + a_1(E_\nu[MeV] - 10) \\
f_B &= \phi_B^{SNO}/\phi_B^{SSM}
\end{aligned}$$

where ϕ_B^{SSM} is the Standard Solar Model prediction to the total Boron neutrino flux.

The χ^2 computation is more straightforward, and we have:

$$\chi_{SNO}^2(f_B, P_{ee}) = \left[\sum_{ij} (f_B r_{SNO}^{th,i} - r_{SNO}^{exp,i}) [\sigma_{SNO}]^{-2} (f_B r_{SNO}^{th,j} - r_{SNO}^{exp,j}) \right]$$

where $r_{SNO}^{exp} = (\phi_B^{SNO}, c_0, c_1, c_2)$ and our theoretical input is $r_{SNO}^{th} = (f_B \phi_B^{SSM}, P_{ee}, 0, 0)$. We disregard the parameters involved in regeneration effect, and then the sum runs in only 4 parameters. σ_{SNO} contains the uncertainties and correlations provided by SNO.

With all taking into account, and minimizing over f_B , we obtain:

$$P_{ee}^{HE} = 0.324 \pm 0.014 \quad (1\sigma) \quad (2)$$

2.1.2 intermediate energy:

The best choice to establish a survival probability for neutrinos with intermediate energy is to use data from Borexino [27]. The collaboration reports a survival probability for the monoenergetic ${}^7\text{Be}$ and pep neutrino fluxes (1σ):

$$P_{ee}({}^7\text{Be}, 0.862 \text{ MeV}) = 0.52 \pm 0.05 \quad ; \quad P_{ee}(pep, 1.44 \text{ MeV}) = 0.43 \pm 0.11 \quad (3)$$

We do not use these values in our analysis, but they are necessary to establish a probability for the low energy neutrinos, calculated in what follows.

2.1.3 low energy:

Using data from Gallex/GNO and Sage it is possible to establish a value for the survival probability for low-energy neutrinos. Since Super-Kamiokande and SNO provides a real-time detection, it is possible to use only data collected during the day, and exclude possible regeneration effects from our analysis. Low-energy solar neutrino experiments does not allow such discrimination, so we rely on the assumption that regeneration effects on Earth does not change the survival probability. This is in accordance to our assumption that any new physics on KamLAND would be subleading, and for the mixing

parameters given by KamLAND no Earth regeneration is expected for low energy neutrinos.

Gallex/GNO and Sage detect neutrinos from all the 8 neutrino sources in the Sun. In the absence of flavour conversions, the fraction of each source on the final detection rate is expected to be:

$$r = (0.561, 2.34 \times 10^{-2}, 4.5 \times 10^{-5}, 0.279, \\ 0.104, 1.32 \times 10^{-2}, 1.837 \times 10^{-2}, 4.8 \times 10^{-4})$$

for neutrinos from the chains (pp, pep, hep, ^7Be , B, C, N, O), respectively. The three main contributions come from pp neutrino, ^7Be neutrinos, ^8B neutrinos and pep neutrinos, in decreasing order. We can use the range for the probabilities for the three last of these contributions discussed at the last section to extract a probability for pp neutrinos. Performing the following χ^2 analysis:

$$\chi_{LE}^2(f_B, P_B, P_{Be}, P_{pep}) = \left[\sum_{ij} (R_i^{th} - R_i^{exp}) [\sigma_{LE}]^{-2} (R_i^{th} - R_i^{exp}) \right] + \\ \left(\frac{P_B - 0.324}{0.014} \right)^2 + \left(\frac{P_{Be} - 0.52}{0.05} \right)^2 + \left(\frac{P_{pep} - 0.43}{0.11} \right)^2$$

we obtain after marginalizing over the free parameters (1σ):

$$P_{ee}^{LE} = 0.57 \pm 0.06 \quad (4)$$

Borexino also reports a survival probability for pp neutrinos fully consistent with our estimation:

$$P_{ee}^{LE}(pp, E < 0.42 \text{ MeV}) = 0.57 \pm 0.09 \quad (1\sigma)$$

leading, in a combined analysis, to a slightly more stringent value:

$$P_{ee}^{LE} = 0.57 \pm 0.05 \quad (5)$$

which we used in what follows.

2.2 Neutrino's mass eigenstates probabilities

For solar neutrinos arriving at the detector during the day (or for low energy neutrinos, in which the Earth regeneration effect can be disregarded), we can

directly replace $P_{i\beta}^{Earth}$ by the corresponding mixing angles:

$$\begin{aligned} P_{ee} &= P_{e1}^{Sun}|U_{1e}|^2 + P_{e2}^{Sun}|U_{2e}|^2 + P_{e3}^{Sun}|U_{3e}|^2 \\ &= c_{13}^2(P_{e1}^{Sun}c_{12}^2 + P_{e2}^{Sun}s_{12}^2) + s_{13}^2P_{e3}^{Sun} \end{aligned}$$

For neutrinos arriving at the detector during the night, we should calculate $P_{i\beta}^{Earth}$.

With KamLAND results on θ_{12} and the recent measurement of θ_{13} by Daya-Bay, Double-Chooz and Reno, we can present an exercise of how much do we know about the physical eigenstates distribution of solar neutrinos in a complete solar model independent way.

By defining the following χ^2 related to low and high-energy solar neutrinos in the following way:

$$\chi_{LE}^2 = \left(\frac{P_{ee}(P_{e1}^{Sun}, P_{e2}^{Sun}, P_{e3}^{Sun} | \theta_{12}, \Delta m_{12}^2) - P_{ee}^{LE}}{\sigma_{LE}} \right)^2 \quad (6)$$

$$\chi_{HE}^2 = \chi_{SK, SNO}^2(P_{e1}, P_{e2}, P_{e2} | \theta_{12}, \Delta m_{12}^2) \quad (7)$$

we performed a statistical analysis through the following χ^2 for low energy solar neutrinos:

$$\begin{aligned} \chi^2(P_{e1}, P_{e2}, P_{e2} | \theta_{12}, \Delta m_{12}^2) &= \chi_{KL}^2(\theta_{12}, \Delta m_{12}^2) + \\ &\quad \left(\frac{P_{ee}(P_{e1}, P_{e2}, P_{e2} | \theta_{12}, \Delta m_{12}^2) - P_{ee}^{LE}}{\sigma_{LE}} \right)^2 \end{aligned}$$

and a similar expression for high energy neutrinos detected during the day.

For high energy neutrinos detected during the night, we calculated:

$$\begin{aligned} \chi^2(P_{e1}, P_{e2}, P_{e2} | \theta_{12}, \Delta m_{12}^2) &= \chi_{KL}^2(\theta_{12}, \Delta m_{12}^2) + \\ &\quad \chi_{SK, SNO}^2(P_{e1}, P_{e2}, P_{e2} | \theta_{12}, \Delta m_{12}^2) \end{aligned}$$

Marginilizing the above χ^2 over the oscillation parameters, we obtain allowed regions for probability transitions to mass eigenstates independent of the flavour conversion mechanism operating in the Sun.

2.2.1 Light-side (normal 12 hierarchy)

First we analyse what are the constrains put on P_{ei}^{Sun} from Solar Neutrino data and KamLAND restricting ourselves to the light-side of the parameter space on θ_{12} ($\theta_{12} \leq \pi/4$). Although this procedure is not completely

solar model independent, the only known mechanism that provides a good explanation to solar neutrino data in the dark region ($\theta_{12} > \pi/4$) involves a strong non-standard interaction, which is disfavoured [28] by recent results on neutrino coherence scattering [29]. Anyway, on the sequence we repeat our analysis for the dark region for completeness.

2.2.2 Low Energy

For low-energy solar neutrinos we can see immediately that the equipartition of mass eigenstates, with $P_{ei} = 1/3$ for all i , is excluded, since it would lead to $P_{ee} = 1/3$. The usual MSW-LMA predicts that the conversion probabilities solution in Sun for lower energy neutrinos are given by their vacuum expressions:

$$\begin{aligned} P_{e1}^{Sun} &= c_{13}^2 c_{12}^2 \\ P_{e2}^{Sun} &= c_{13}^2 s_{12}^2 \\ P_{e3}^{Sun} &= s_{13}^2 \end{aligned}$$

leading to:

$$P_{ee} = c_{13}^4 (c_{12}^4 + s_{12}^4) + s_{13}^4 = c_{13}^4 (1 - 0.5 \sin^2(2\theta_{12})) + s_{13}^4$$

In fig. 1 we can see in blue the allowed region for the values for the conversion probabilities P_{ei} given by the low-energy solar neutrino experiments. The MSW-LMA prediction is marked with an upper triangle.

2.2.3 High Energy

For high-energy neutrinos the Earth matter induces changes in the probabilities, and we have:

$$P_{ee} = P_{e1}^{Sun} P_{1e}^{Earth} + P_{e2}^{Sun} P_{2e}^{Earth} + P_{e3}^{Sun} P_{3e}^{Earth}$$

where P_{ie}^{Earth} depends on both the oscillation parameters and the neutrino energy. So even if the probabilities P_{ei} are constant, we obtain an energy dependent probability for neutrinos arriving at the detector during the night.

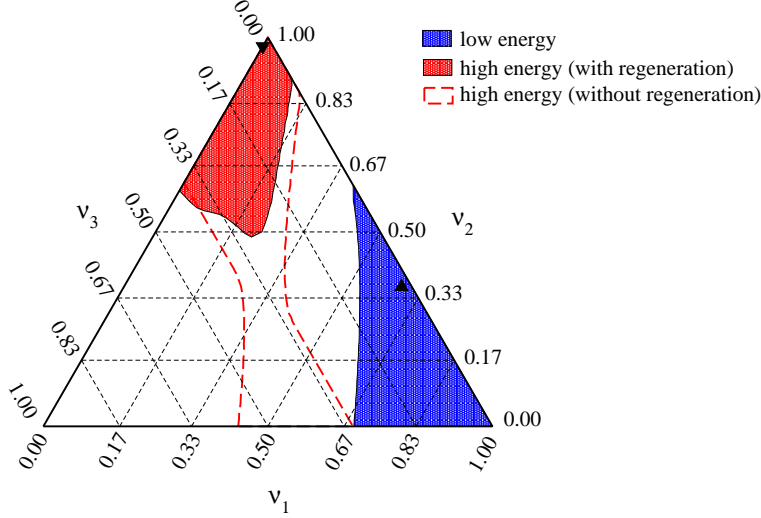


Figure 1: The allowed region for the conversion probabilities P_{ei} for low-energy solar neutrinos (blue) and high-energy solar neutrinos (read). In dashed read we exclude the data from day-night asymmetry from the analysis. We restricted the analysis for the region $\theta_{12} \leq \pi/4$.

For neutrinos arriving during the day, we have the similar expression for low-energy neutrinos:

$$P_{ee} = c_{13}^2(P_{e1}^{Sun}c_{12}^2 + P_{e2}^{Sun}s_{12}^2) + s_{13}^2P_{e3}^{Sun} = 0.324 \pm 0.014$$

Unlike low energy neutrinos, an equipartition of probabilities is possible, since $P_{ee} = 1/3$ is inside 1σ range. In fig 1 we present the allowed regions for solar probabilities of day high-energy neutrinos in dashed red.

When we include the night high-energy data, the regeneration effects exclude a large portion of allowed region. In particular, equipartition predicts a vanishing regeneration effect, disfavoured by experimental data, as can be seen in the filled red region in fig 1.

If we rewrite the survival probability during the day assuming that $P_{e3}^{Earth} = \sin^2 \theta_{13}$, which is a very good assumption for the oscillation parameters stabilised by KamLAND, we have for the survival probability during the night:

$$P_{ee}^N = P_{e1}^{Sun}P_{1e}^{Earth} + P_{e2}^{Sun}P_{2e}^{Earth} + P_{e3}^{Sun}\sin^2 \theta_{13}$$

Also, we have that P_{2e}^{Earth} is always larger than $U_{2e} = \cos^2 \theta_{13} \sin^2 \theta_{12}$, the asymptotic value when the matter interactions is negligible. Then, to have a negative day-night asymmetry, we will need:

$$P_{e2}^{Sun} > P_{e1}^{Sun}$$

then excluding the portion of fig 1 that splits the triangle from the lower left corner to the middle of the right edge.

Performing a χ^2 analysis with the full data sample for the high-energy experiments Super-Kamiokande and SNO, using the same χ^2 used in section 2.1.1, we present in fig. 1 in red the allowed region for high-energy neutrinos.

The MSW-LMA mechanism predicts that the high energy neutrinos, which fully felt the resonance, leaves the Sun as a pure ν_2 state (with a small fraction of ν_3 due to non-vanishing θ_{13}), and is depicted as a lower triangle.

2.3 Dark side

In fig. (2) we present the results on the Dark-side of neutrino parameter space. If it was not for the regeneration effect, the two situations were equivalent to an exchange between ν_1 and ν_2 . With regeneration effect, the equivalence is broken, and we get the allowed regions depicted in 2.

In the next section we present how these informations can be used to arrive at a first constraint on new physics acting on solar neutrinos.

3 Decoherence and Relaxation effects on Probabilities

Having constraints on the incoherent admixture of mass eigenstates that composes the solar neutrino flux, it is possible to set a limit on any conversion mechanisms that alter such admixture. As can be found in several other references (for an incomplete list, see [30–40]), if neutrinos are considered as a subsystem that interacts with an environment in the Open Quantum System framework, possible modifications on neutrino conversion probabilities can be induced. As we focus in conversion between mass eigenstates, we choosed to present in a succinct way the main steps for arriving at such probabilities.

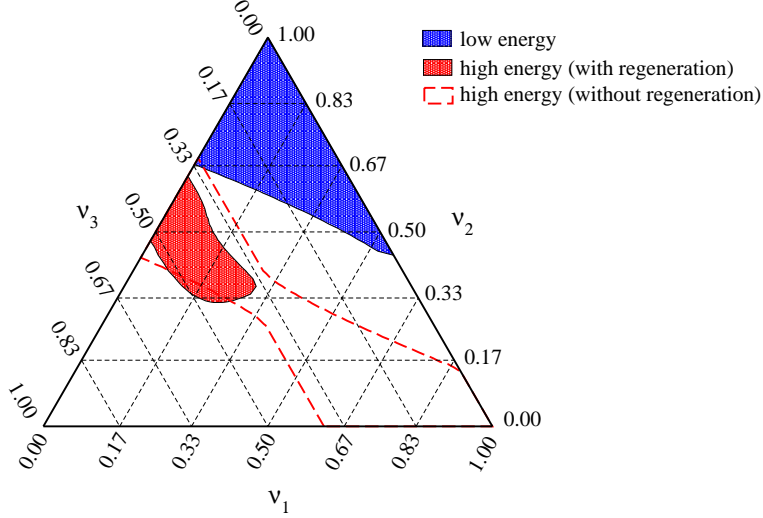


Figure 2: Same as fig. 1 but for the dark region, $\theta_{12} > \pi/2$.

More details on the the procedure to obtain the conversion probabilities can be found on Appendix.

Starting with Lindblad generator, the density matrix dynamics can be expressed through the following evolution equation:

$$\frac{d\rho(t)}{dt} = -i[H, \rho(t)] + D(\rho) \quad , \quad (8)$$

where $\rho(t)$ is the usual density matrix, H is the Hamiltonian and

$$D(\rho) = +\frac{1}{2} \sum_{p=1}^{N^2-1} ([V_p, \rho(t)V_p^\dagger] + [V_p\rho(t), V_p^\dagger]) \quad , \quad (9)$$

with V being a hermetian matrix to ensure that the system's entropy increases with time.

To solve the evolution equation it is convenient to expand it using $SU(3)$ generators and rewrite eq. (8) in terms of the expansion coefficients. Most of the interesting phenomenological consequences of decoherence effects can be found with a diagonal $D(\rho)$ on such expansion, a choice that also guarantees complete positivity. After some algebra, we find that the matrix D , with the mentioned simplifying choices, can be fully parameterized as:

$$D_{11} = \Gamma_1 + \Gamma_8/3 + \gamma_{12}$$

$$\begin{aligned}
D_{22} &= \Gamma_2 + \Gamma_8/3 + \gamma_{12} \\
D_{33} &= \Gamma_3 + \Gamma_8/3 \\
D_{44} &= \Gamma_3/4 + \Gamma_4 + \gamma_{13} \\
D_{55} &= \Gamma_3/4 + \Gamma_5 + \gamma_{13} \\
D_{66} &= \Gamma_3/4 + \Gamma_6 + \gamma_{23} \\
D_{77} &= \Gamma_3/4 + \Gamma_7 + \gamma_{23} \\
D_{88} &= \Gamma_8
\end{aligned} \tag{10}$$

where the Γ 's are the parameters that induce relaxation effects, and must obey the following constraints:

$$\begin{aligned}
\Gamma_3 &= \Gamma_1 + \Gamma_2 \\
\Gamma_8 &= \frac{1}{2}(\Gamma_4 + \Gamma_5 + \Gamma_6 + \Gamma_7)
\end{aligned}$$

while the γ 's induce decoherence effects, and must obey the following constraints:

$$\sqrt{2\gamma_{13}} + \sqrt{2\gamma_{23}} = \sqrt{2\gamma_{12}}$$

or any interchange between the γ 's.

In this work we focus in the solar neutrino flux partition on mass eigenstates, so it is convenient to calculate the mass eigenstates conversion probabilities. After some algebra (shown in appendix), we obtain that such probabilities depend only on the independent parameters Γ_3 and Γ_8 , through:

$$\begin{aligned}
P_{11} = P_{22} &= \frac{1}{3} + \frac{1}{2} \exp \left[- \left(\Gamma_3 + \frac{\Gamma_8}{3} \right) t \right] + \frac{1}{6} \exp[-\Gamma_8 t] \\
P_{12} = P_{21} &= \frac{1}{3} - \frac{1}{2} \exp \left[- \left(\Gamma_3 + \frac{\Gamma_8}{3} \right) t \right] + \frac{1}{6} \exp[-\Gamma_8 t] \\
P_{13} = P_{23} = P_{31} = P_{32} &= \frac{1}{3} - \frac{1}{3} \exp[-\Gamma_8 t] \\
P_{33} &= \frac{1}{3} + \frac{2}{3} \exp[-\Gamma_8 t]
\end{aligned} \tag{11}$$

As it expected, when $\Gamma_{3,8} \rightarrow 0$, no transition between mass eigenstates are induced, and the system evolves adiabatically. In the other extreme, for very large values of Γ_3 and Γ_8 , $P_{ij} \rightarrow 1/3$ for any i, j , and a complete equipartition on mass eigenstates is produced independent on the initial content of solar neutrino flux.

4 Results

In this section I will present the limits obtained on the new physics parameters, first with no assumption on the flavour physics at play inside the Sun, and then through a complete analysis of solar neutrino data assuming that the LMA-MSW flavour conversion mechanism as the leading effect acting on the neutrinos.

4.1 No assumption on flavour conversion

As discussed in Sec. 2.2, fig. 1 establishes the limits on the mass eigenstates distribution on solar neutrino flux without any assumption on the neutrino flavour conversion mechanism inside the Sun. It is then straightforward to convert these constraints on limits in any new mechanism that induces conversion between mass eigenstates. For instance, since a perfect equipartition is excluded to more than 3σ , such exclusion can be converted into limits on the parameters Γ_3 and Γ_8 .

Introducing the probabilities presented in Eq.(11) into Eq.(1) and performing the same statistical analysis used in Sec.2 with two extra parameters, we obtain, after minimizing over all the remaining parameters, an allowed region for the OQS parameters. We present such region at fig. 3.

Presenting the limits one at a time, it is possible to establish, without any assumptions on flavour conversion of solar neutrinos inside the Sun, the following limits at 1σ (3σ):

$$\Gamma_3 < 1.7 (7.2) \times 10^{-19} \text{ eV} \quad ; \quad \Gamma_8 < 2.2 (15.0) \times 10^{-19} \text{ eV} . \quad (12)$$

4.2 Complete statistical analysis

The exercise presented in previous sections consists of a very robust way to limit new physics on neutrino sector from neutrino flux produced in astrophysics objects, where it is expected that the neutrinos arrive at Earth as an incoherent admixture of mass eigenstates, and the uncertainties on the initial neutrino flux are large. For solar neutrinos, only the first of these statements applies, so we can proceed a further step and include our knowledge on flavour conversion inside the Sun to establish a stronger bound on

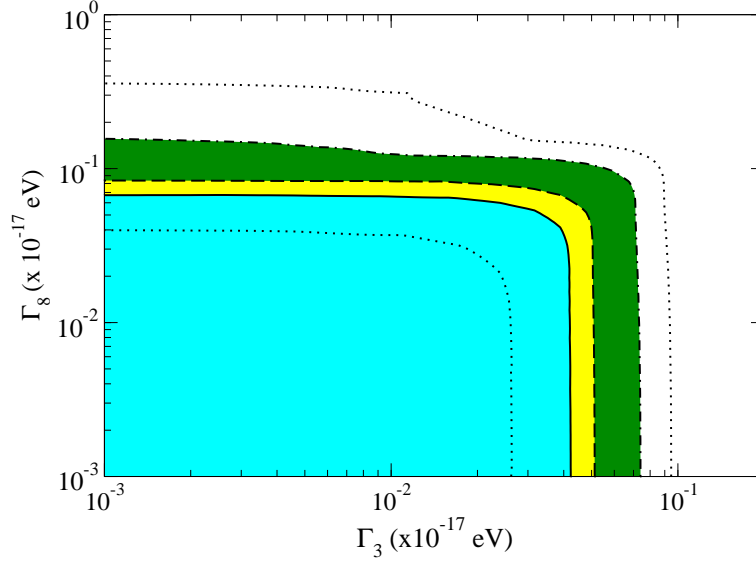


Figure 3: Allowed region on parameters Γ_3 and Γ_8 with no assumption on flavour conversion physics inside the Sun. The different regions correspond to 1σ (dotted), 90% C.L. (straight line), 95% C.L. (long-dashed), 99% C.L. (dot-dashed) and 3σ (dotted).

the new physics analysed here. We present in this section the results of such analysis.

For the solar neutrino data, we perform a statistical analysis with the full spectral data from Super-Kamiokande phases I, III and IV [23–25], the combined analysis of all three SNO phases [26], Borexino [27], combined Gallex+GNO [41], SAGE [42] and Homestake [43]. For KamLAND data we used their 2008 spectral data [44].

The statistical procedure follows the same one presented in previous articles [45, 46], with two free parameters related to standard neutrino parameters, Δm_{21}^2 and θ_{12} , and two new free parameters related to new physics, Γ_3 and Γ_8 . The mixing angle θ_{13} is fixed at the best fit point of a global analysis [47].

After minimizing over the standard neutrino parameters, we obtain the allowed region shown in fig. 4. We obtain a slight enhancement on the limits in the non-standard parameters when we use the full knowledge of the neutrino evolution inside the Sun.

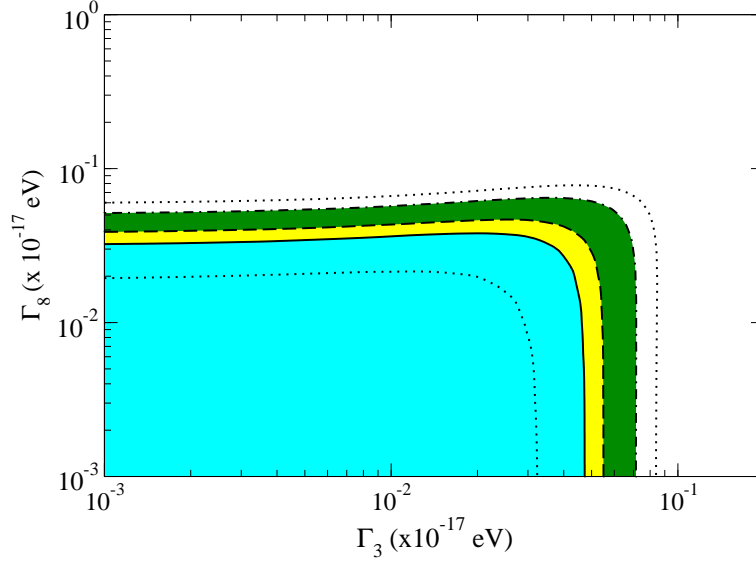


Figure 4: Allowed region on parameters Γ_3 and Γ_8 using the full knowledge of MSW effect inside the Sun. The different regions correspond to 1σ (dotted), 90% C.L. (straight line), 95% C.L. (long-dashed), 99% C.L. (dot-dashed) and 3σ (dotted).

Presenting the limits one at a time, the solar neutrinos + KamLAND data provide the following limits at 1σ (3σ):

$$\Gamma_3 < 1.1 (6.5) \times 10^{-19} \text{eV} \quad ; \quad \Gamma_8 < 2.1 (7.1) \times 10^{-19} \text{eV} . \quad (13)$$

5 Conclusions

We presented in this work a novel procedure to analyse the neutrino flux coming from astrophysical objects, focusing on the mass eigenstates partition, since it is expected that the neutrino flux arrives as an incoherent admixture of such eigenstates. Using solar neutrino flux data, we inferred the limits on relaxation parameters in a Open Quantum System formalism with no assumptions on the neutrino flavour physics inside the Sun. When compared with limits obtained with full knowledge of solar neutrino production and MSW flavour conversion mechanism, the limits could be only slightly enhanced, demonstrating that the analysis with no assumptions on flavour conversion mechanism inside the Sun is quite robust. We pretend to use

this kind of analysis in other astrophysical objects, such as supernovae and high-energy neutrino sources, where the uncertainty of neutrino production and flavour conversion mechanisms are uncertain.

Acknowledgements

Work partially supported by CNPq (grant no. 310952/2018-2) and FAPESP (grant no. 2014/19164-6 and no. 2019/15600-0). The author would like to thank D. R. Gratieri and R. L. N. Oliveira, with whom discussions on the early stage of the work were fundamental to its production.

References

- [1] J. N. Bahcall, “Solar neutrinos. I: Theoretical,” *Phys. Rev. Lett.*, vol. 12, pp. 300–302, 1964. [,9(1964)].
- [2] J. N. Bahcall and R. Davis, “Solar Neutrinos - a Scientific Puzzle,” *Science*, vol. 191, pp. 264–267, 1976. [,141(1976)].
- [3] A. I. Abazov *et al.*, “Search for neutrinos from sun using the reaction Ga-71 (electron-neutrino e^-) Ge-71,” *Phys. Rev. Lett.*, vol. 67, pp. 3332–3335, 1991.
- [4] P. Anselmann *et al.*, “Implications of the GALLEX determination of the solar neutrino flux,” *Phys. Lett.*, vol. B285, pp. 390–397, 1992.
- [5] K. S. Hirata *et al.*, “Observation of B-8 Solar Neutrinos in the Kamiokande-II Detector,” *Phys. Rev. Lett.*, vol. 63, p. 16, 1989.
- [6] Y. Fukuda *et al.*, “Measurements of the solar neutrino flux from Super-Kamiokande’s first 300 days,” *Phys. Rev. Lett.*, vol. 81, pp. 1158–1162, 1998. [Erratum: *Phys. Rev. Lett.* 81, 4279(1998)].
- [7] Q. R. Ahmad *et al.*, “Measurement of the rate of $\nu_e + d \rightarrow p + p + e^-$ interactions produced by ^8B solar neutrinos at the Sudbury Neutrino Observatory,” *Phys. Rev. Lett.*, vol. 87, p. 071301, 2001.

- [8] B. Pontecorvo, “Neutrino Experiments and the Problem of Conservation of Leptonic Charge,” *Sov. Phys. JETP*, vol. 26, pp. 984–988, 1968. [Zh. Eksp. Teor. Fiz.53,1717(1967)].
- [9] L. Wolfenstein, “Neutrino oscillations in matter,” *Phys. Rev. D*, vol. 17, pp. 2369–2374, May 1978.
- [10] S. P. Mikheyev and A. Yu. Smirnov, “Resonance Amplification of Oscillations in Matter and Spectroscopy of Solar Neutrinos,” *Sov. J. Nucl. Phys.*, vol. 42, pp. 913–917, 1985. [,305(1986)].
- [11] S. P. Mikheyev and A. Y. Smirnov, “Resonant amplification of ν oscillations in matter and solar-neutrino spectroscopy,” *Il Nuovo Cimento C*, vol. 9, pp. 17–26, Jan 1986.
- [12] A. M. Gago, M. M. Guzzo, P. C. de Holanda, H. Nunokawa, O. L. G. Peres, V. Pleitez, and R. Zukanovich Funchal, “Global analysis of the postSNO solar neutrino data for standard and nonstandard oscillation mechanisms,” *Phys. Rev.*, vol. D65, p. 073012, 2002.
- [13] K. Eguchi *et al.*, “First results from KamLAND: Evidence for reactor anti-neutrino disappearance,” *Phys. Rev. Lett.*, vol. 90, p. 021802, 2003.
- [14] P. F. de Salas, D. V. Forero, C. A. Ternes, M. Tortola, and J. W. F. Valle, “Status of neutrino oscillations 2018: 3σ hint for normal mass ordering and improved CP sensitivity,” *Phys. Lett.*, vol. B782, pp. 633–640, 2018.
- [15] I. Esteban, M. C. Gonzalez-Garcia, A. Hernandez-Cabezudo, M. Maltoni, and T. Schwetz, “Global analysis of three-flavour neutrino oscillations: synergies and tensions in the determination of θ_{23} , δ_{cp} , and the mass ordering,” *Journal of High Energy Physics*, vol. 2019, p. 106, Jan 2019.
- [16] M. P. Decowski, “KamLAND’s precision neutrino oscillation measurements,” *Nucl. Phys.*, vol. B908, pp. 52–61, 2016.
- [17] D. Adey *et al.*, “Measurement of the Electron Antineutrino Oscillation with 1958 Days of Operation at Daya Bay,” *Phys. Rev. Lett.*, vol. 121, no. 24, p. 241805, 2018.

- [18] G. Bak *et al.*, “Measurement of Reactor Antineutrino Oscillation Amplitude and Frequency at RENO,” *Phys. Rev. Lett.*, vol. 121, no. 20, p. 201801, 2018.
- [19] Y. Abe *et al.*, “Improved measurements of the neutrino mixing angle θ_{13} with the Double Chooz detector,” *JHEP*, vol. 10, p. 086, 2014. [Erratum: JHEP02,074(2015)].
- [20] J. N. Bahcall, A. M. Serenelli, and S. Basu, “New solar opacities, abundances, helioseismology, and neutrino fluxes,” *Astrophys. J.*, vol. 621, pp. L85–L88, 2005.
- [21] N. Vinyoles, A. M. Serenelli, F. L. Villante, S. Basu, J. Bergström, M. C. Gonzalez-Garcia, M. Maltoni, C. Peña-Garay, and N. Song, “A new Generation of Standard Solar Models,” *Astrophys. J.*, vol. 835, no. 2, p. 202, 2017.
- [22] P. C. de Holanda and A. Yu. Smirnov, “Homestake result, sterile neutrinos and low-energy solar neutrino experiments,” *Phys. Rev.*, vol. D69, p. 113002, 2004.
- [23] J. Hosaka *et al.*, “Solar neutrino measurements in super-Kamiokande-I,” *Phys. Rev.*, vol. D73, p. 112001, 2006.
- [24] S. Fukuda *et al.*, “Determination of solar neutrino oscillation parameters using 1496 days of Super-Kamiokande I data,” *Phys. Lett.*, vol. B539, pp. 179–187, 2002.
- [25] K. Abe *et al.*, “Solar Neutrino Measurements in Super-Kamiokande-IV,” *Phys. Rev.*, vol. D94, no. 5, p. 052010, 2016.
- [26] B. Aharmim *et al.*, “Combined Analysis of all Three Phases of Solar Neutrino Data from the Sudbury Neutrino Observatory,” *Phys. Rev.*, vol. C88, p. 025501, 2013.
- [27] M. Agostini *et al.*, “Comprehensive measurement of pp -chain solar neutrinos,” *Nature*, vol. 562, no. 7728, pp. 505–510, 2018.
- [28] I. Esteban, M. C. Gonzalez-Garcia, M. Maltoni, I. Martinez-Soler, and J. Salvado, “Updated Constraints on Non-Standard Interactions from Global Analysis of Oscillation Data,” *JHEP*, vol. 08, p. 180, 2018.

- [29] D. Akimov *et al.*, “Observation of Coherent Elastic Neutrino-Nucleus Scattering,” *Science*, vol. 357, no. 6356, pp. 1123–1126, 2017.
- [30] R. L. N. Oliveira and M. M. Guzzo, “Dissipation and θ_{13} in neutrino oscillations,” *Eur. Phys. J.*, vol. C73, p. 2434, 2013.
- [31] M. M. Guzzo, P. C. de Holanda, and R. L. N. Oliveira, “Quantum Dissipation in a Neutrino System Propagating in Vacuum and in Matter,” *Nucl. Phys.*, vol. B908, pp. 408–422, 2016.
- [32] G. Balieiro Gomes, M. M. Guzzo, P. C. de Holanda, and R. L. N. Oliveira, “Parameter Limits for Neutrino Oscillation with Decoherence in KamLAND,” *Phys. Rev.*, vol. D95, no. 11, p. 113005, 2017.
- [33] G. L. Fogli, E. Lisi, A. Marrone, D. Montanino, and A. Palazzo, “Probing non-standard decoherence effects with solar and KamLAND neutrinos,” *Phys. Rev.*, vol. D76, p. 033006, 2007.
- [34] R. L. N. Oliveira and M. M. Guzzo, “Quantum dissipation in vacuum neutrino oscillation,” *Eur. Phys. J.*, vol. C69, pp. 493–502, 2010.
- [35] J. A. B. Coelho, W. A. Mann, and S. S. Bashar, “Nonmaximal θ_{23} mixing at NOvA from neutrino decoherence,” *Phys. Rev. Lett.*, vol. 118, no. 22, p. 221801, 2017.
- [36] R. L. N. Oliveira, “Dissipative Effect in Long Baseline Neutrino Experiments,” *Eur. Phys. J.*, vol. C76, no. 7, p. 417, 2016.
- [37] J. A. B. Coelho and W. A. Mann, “Decoherence, matter effect, and neutrino hierarchy signature in long baseline experiments,” *Phys. Rev.*, vol. D96, no. 9, p. 093009, 2017.
- [38] R. L. N. de Oliveira, M. M. Guzzo, and P. C. de Holanda, “Quantum Dissipation and CP Violation in MINOS,” *Phys. Rev.*, vol. D89, no. 5, p. 053002, 2014.
- [39] J. A. Carpio, E. Massoni, and A. M. Gago, “Revisiting quantum decoherence for neutrino oscillations in matter with constant density,” *Phys. Rev.*, vol. D97, no. 11, p. 115017, 2018.

- [40] P. Coloma, J. Lopez-Pavon, I. Martinez-Soler, and H. Nunokawa, “Decoherence in Neutrino Propagation Through Matter, and Bounds from IceCube/DeepCore,” *Eur. Phys. J.*, vol. C78, no. 8, p. 614, 2018.
- [41] F. Kaether, W. Hampel, G. Heusser, J. Kiko, and T. Kirsten, “Reanalysis of the GALLEX solar neutrino flux and source experiments,” *Phys. Lett.*, vol. B685, pp. 47–54, 2010.
- [42] J. N. Abdurashitov *et al.*, “Measurement of the solar neutrino capture rate with gallium metal. III: Results for the 2002–2007 data-taking period,” *Phys. Rev.*, vol. C80, p. 015807, 2009.
- [43] B. T. Cleveland, T. Daily, R. Davis, Jr., J. R. Distel, K. Lande, C. K. Lee, P. S. Wildenhain, and J. Ullman, “Measurement of the solar electron neutrino flux with the Homestake chlorine detector,” *Astrophys. J.*, vol. 496, pp. 505–526, 1998.
- [44] S. Abe *et al.*, “Precision Measurement of Neutrino Oscillation Parameters with KamLAND,” *Phys. Rev. Lett.*, vol. 100, p. 221803, 2008.
- [45] P. C. de Holanda, “Possible scenario for MaVaN’s as the only neutrino flavor conversion mechanism in the Sun,” *JCAP*, vol. 0907, p. 024, 2009.
- [46] P. C. de Holanda and A. Yu. Smirnov, “Solar neutrinos: The SNO salt phase results and physics of conversion,” *Astropart. Phys.*, vol. 21, pp. 287–301, 2004.
- [47] I. Esteban, M. C. Gonzalez-Garcia, A. Hernandez-Cabezudo, M. Maltoni, and T. Schwetz, “Global analysis of three-flavour neutrino oscillations: synergies and tensions in the determination of θ_{23} , δ_{CP} , and the mass ordering,” *JHEP*, vol. 01, p. 106, 2019.

A OQF Formalism

It is possible to write the decoherence operator in eq.(9) as:

$$D(\rho) = +\frac{1}{2} \sum_{p=1}^{N^2-1} [[V_p, \rho(t)], V_p]$$

Expanding using Gell-Mann matrices:

$$V_p = v_{pi}\lambda_i \quad ; \quad \rho = \rho_j\lambda_j$$

we have:

$$D(\rho) = +\frac{1}{2} \sum_{p,i,j,k} v_{pi}v_{pk}\rho_j[[\lambda_i, \lambda_j], \lambda_k]$$

and using the SU(3) structure constants:

$$\left[\frac{\lambda_i}{2}, \frac{\lambda_j}{2} \right] = f_{ijk} \frac{\lambda_k}{2}$$

we have (with sumation implicit):

$$D(\rho) = +v_{pi}v_{pk}\rho_j f_{ijl}[\lambda_l, \lambda_k] = +2v_{pi}v_{pk}\rho_j f_{ijl}f_{lkm}\lambda_m$$

Finally, writing the evolution equation in terms of a system on ρ_i 's:

$$\frac{d\rho_l}{dt} = (...) + D_{jm}\rho_j$$

where

$$D_{jm} = 2v_{pi}v_{pk}f_{ijl}f_{kml}$$

Replacing the SU(3) structure constants:

$$f^{123} = 1 \quad ; \quad f^{147} = f^{165} = f^{246} = f^{257} = f^{345} = f^{376} = \frac{1}{2} \quad ; \quad f^{458} = f^{678} = \frac{\sqrt{3}}{2}$$

we have for the diagonal entries:

$$D_{11} = 2 \sum_{p,i,l} (v_{pi})^2 (f_{i1l})^2$$

Replacing all non-null entries:

$$D_{11} = 2 \sum_p \left((v_{p2})^2 + (v_{p3})^2 + \frac{1}{4}(v_{p4})^2 + \frac{1}{4}(v_{p5})^2 + \frac{1}{4}(v_{p6})^2 + \frac{1}{4}(v_{p7})^2 \right)$$

Renaming:

$$\vec{a}_i = (\{v_{pi}\}, p = 1, 8)$$

we obtain:

$$D_{11} = 2a_2^2 + 2a_3^2 + \frac{1}{2}a_4^2 + \frac{1}{2}a_5^2 + \frac{1}{2}a_6^2 + \frac{1}{2}a_7^2$$

and, similarly:

$$D_{22} = 2a_1^2 + 2a_3^2 + \frac{1}{2}a_4^2 + \frac{1}{2}a_5^2 + \frac{1}{2}a_6^2 + \frac{1}{2}a_7^2$$

$$D_{33} = 2a_1^2 + 2a_2^2 + \frac{1}{2}a_4^2 + \frac{1}{2}a_5^2 + \frac{1}{2}a_6^2 + \frac{1}{2}a_7^2$$

$$D_{88} = \frac{3}{2} (a_4^2 + a_5^2 + a_6^2 + a_7^2)$$

For the 44 element:

$$D_{44} = 2v_{pi}v_{pk}f_{i4l}f_{k4l}$$

we have (renaming $\sqrt{3}a_8 \rightarrow a_8$):

$$\begin{aligned} D_{44} &= \frac{1}{2} (a_1^2 + a_2^2 + a_3^2 + a_5^2 + a_6^2 + a_7^2) + \frac{3}{2} (a_5^2 + a_8^2) + 4v_{p3}v_{p8} \frac{\sqrt{3}}{4} \\ &= \frac{1}{2} (a_1^2 + a_2^2 + 4a_5^2 + a_6^2 + a_7^2) + \frac{1}{2} (\vec{a}_3 + \vec{a}_8)^2 \end{aligned}$$

and, similarly:

$$D_{55} = \frac{1}{2} (a_1^2 + a_2^2 + 4a_4^2 + a_6^2 + a_7^2) + \frac{1}{2} (\vec{a}_3 + \vec{a}_8)^2$$

$$D_{66} = \frac{1}{2} (a_1^2 + a_2^2 + a_4^2 + a_5^2 + 4a_7^2) + \frac{1}{2} (\vec{a}_3 - \vec{a}_8)^2$$

$$D_{77} = \frac{1}{2} (a_1^2 + a_2^2 + a_4^2 + a_5^2 + 4a_6^2) + \frac{1}{2} (\vec{a}_3 - \vec{a}_8)^2$$

Having only decoherence, and no relaxation, it is possible to show that:

$$a_1 = a_2 = a_4 = a_5 = a_6 = a_7 = 0$$

and we renamed the non-vanishing parameters as:

$$\begin{aligned} D_{11} = D_{22} &= 2a_3^2 = \gamma_{12} \\ D_{44} = D_{55} &= \frac{1}{2} (\vec{a}_3 + \vec{a}_8)^2 = \gamma_{13} \\ D_{66} = D_{77} &= \frac{1}{2} (\vec{a}_3 - \vec{a}_8)^2 = \gamma_{23} \end{aligned}$$

For colinear \vec{a}_3 and \vec{a}_8 the following constraint are obtained:

$$\sqrt{2\gamma_{13}} + \sqrt{2\gamma_{23}} = \sqrt{2\gamma_{12}}$$

or any interchange between the γ 's.

Introducing relaxation, a convenient nomenclature would be to set:

$$\begin{aligned}\Gamma_1 &= 2a_2^2 \\ \Gamma_2 &= 2a_1^2 \\ \Gamma_3 &= 2a_1^2 + 2a_2^2 \\ \Gamma_4 &= 2a_5^2 + \frac{1}{2}(a_6^2 + a_7^2) \\ \Gamma_5 &= 2a_4^2 + \frac{1}{2}(a_6^2 + a_7^2) \\ \Gamma_6 &= \frac{1}{2}(a_4^2 + a_5^2) + 2a_7^2 \\ \Gamma_7 &= \frac{1}{2}(a_4^2 + a_5^2) + 2a_6^2 \\ \Gamma_8 &= \frac{3}{2}(a_4^2 + a_5^2 + a_6^2 + a_7^2)\end{aligned}$$

and with this choice we obtain:

$$\begin{aligned}D_{11} &= \Gamma_1 + \Gamma_8/3 + \gamma_{12} \\ D_{22} &= \Gamma_2 + \Gamma_8/3 + \gamma_{12} \\ D_{33} &= \Gamma_3 + \Gamma_8/3 \\ D_{44} &= \Gamma_3/4 + \Gamma_4 + \gamma_{13} \\ D_{55} &= \Gamma_3/4 + \Gamma_5 + \gamma_{13} \\ D_{66} &= \Gamma_3/4 + \Gamma_6 + \gamma_{23} \\ D_{77} &= \Gamma_3/4 + \Gamma_7 + \gamma_{23} \\ D_{88} &= \Gamma_8\end{aligned}$$

where the Γ 's must obey the following constraints:

$$\begin{aligned}\Gamma_3 &= \Gamma_1 + \Gamma_2 \\ \Gamma_8 &= \frac{1}{2}(\Gamma_4 + \Gamma_5 + \Gamma_6 + \Gamma_7)\end{aligned}$$

To calculate survival probabilities, we use:

$$P_{\alpha\beta} = \sum_i 2\rho_{i,\alpha}(0)\rho_{i,\beta}(t)$$

and to focus on conversion probabilities between mass eigenstates, we would use:

$$\begin{aligned}
\nu_1 &: \rho_0 = \frac{1}{\sqrt{6}} \quad ; \quad \rho_3 = +\frac{1}{2} \quad ; \quad \rho_8 = +\frac{1}{2\sqrt{3}} \\
\nu_2 &: \rho_0 = \frac{1}{\sqrt{6}} \quad ; \quad \rho_3 = -\frac{1}{2} \quad ; \quad \rho_8 = +\frac{1}{2\sqrt{3}} \\
\nu_3 &: \rho_0 = \frac{1}{\sqrt{6}} \quad ; \quad \rho_3 = 0 \quad ; \quad \rho_8 = -\frac{1}{\sqrt{3}}
\end{aligned}$$

Working on diagonal basis, where $H = h_3\lambda_3 + h_8\lambda_8$ is easy to see that the evolution of ρ_3 and ρ_8 are completely decoupled, and then:

$$\begin{aligned}
\rho_3(t) &= \exp\left[-\left(\Gamma_3 + \frac{\Gamma_8}{3}\right)t\right] \rho_3(0) \\
\rho_8(t) &= \exp[-\Gamma_8 t] \rho_8(0)
\end{aligned}$$

which leaves to:

$$\begin{aligned}
P_{11} = P_{22} &= \frac{1}{3} + \frac{1}{2} \exp\left[-\left(\Gamma_3 + \frac{\Gamma_8}{3}\right)t\right] + \frac{1}{6} \exp[-\Gamma_8 t] \\
P_{12} = P_{21} &= \frac{1}{3} - \frac{1}{2} \exp\left[-\left(\Gamma_3 + \frac{\Gamma_8}{3}\right)t\right] + \frac{1}{6} \exp[-\Gamma_8 t] \\
P_{13} = P_{23} = P_{31} = P_{32} &= \frac{1}{3} - \frac{1}{3} \exp[-\Gamma_8 t] \\
P_{33} &= \frac{1}{3} + \frac{2}{3} \exp[-\Gamma_8 t]
\end{aligned}$$